TOXICOLOGIC PATHOLOGY, vol 30, no 2, pp 209–215, 2002

Distribution of Inorganic Mercury in Liver and Kidney of Beluga and Bowhead Whales Through Autometallographic Development of Light Microscopic Tissue Sections

VICTORIA M. WOSHNER,[1,2] TODD M. O'HARA,[1] JO ANN EURELL,[2] MATTHEW A. WALLIG,[3] GERALD R. BRATTON,[4] ROBERT S. SUYDAM,[1] AND VAL R. BEASLEY[2]

[1]*Department of Wildlife Management, North Slope Borough, Barrow, Alaska 99723, USA*
[2]*Department of Veterinary Biosciences, University of Illinois, Urbana, Illinois 61802, USA*
[3]*Department of Veterinary Pathobiology, University of Illinois, Urbana, Illinois 61802, USA, and*
[4]*Department of Veterinary Anatomy and Public Health, Texas A&M University, College Station, Texas 77843, USA*

ABSTRACT

Inorganic mercury was localized through autometallography (AMG) in kidney and liver of free-ranging, subsistence-harvested beluga (*Delphinapterus leucas*; n = 20) and bowhead (*Balaena mysticetus*; n = 5) whales. AMG granules were not evident in bowhead tissues, confirming nominal mercury (Hg) concentrations (range = 0.011 to 0.038 ug/g ww for total Hg). In belugas, total Hg ranged from 0.30 to 17.11 and from 0.33 to 82.47 ug/g ww in liver and kidney, respectively. AMG granules were restricted to cortical tubular epithelial cytoplasm in belugas with lower tissue burdens; whales with higher tissue burdens had granules throughout the uriniferous tubular epithelium. In liver, AMG granular densities differed between lobular zones, concentrating in stellate macrophages and bile cannalicular domains of hepatocytes. AMG granules aggregated in periportal regions in belugas with lower hepatic Hg concentrations, yet among whales with higher Hg, AMG granule deposition extended to pericentral and midzonal regions of liver lobules. Mean areas occupied by AMG granules correlated well with hepatic Hg concentrations and age. In beluga livers, AMG staining density was not associated with lipofuscin quantity (an index of oxidative damage). Occasionally, AMG granules and lipofuscin were colocalized, but more often were not, implying that Hg was not a prominent factor in hepatic lipofuscin deposition in belugas.

Keywords. Autometallography; *Balaena mysticetus*; *Delphinapterus leucas*; histochemistry; lipofuscin.

INTRODUCTION

The propensity for various marine mammal species to accumulate some inorganic elements, particularly mercury (Hg), in tissues to concentrations associated with toxicosis in domestic species (3, 25, 40, 42, 43, 45, 46) has provoked conjecture as to the potential adverse effects of these residues (5). X-ray microanalytic evidence has provided support for the theory that the hepatic mercury (Hg) to selenium (Se) molar ratio of 1:1 first noted by Koeman (24) in marine mammals arises from deposition of tiemannite (mercuric selenide) crystals as an end product of methylmercury detoxification (28, 29).

Postmortem examination of Atlantic bottlenose dolphins (*Tursiops truncatus*) stranded along the coast of Florida revealed abundant lipofuscin deposition (identified through a nonlipofuscin specific Schmorl stain) in portal areas of the liver as well as in proximal tubular cells of the kidney, which appeared to be age-correlated (31). Four of 9 animals with hepatic lipofuscinosis had histologic evidence of hepatic degeneration or inflammation. Electron microscopy with energy dispersive X-ray analysis (EDAX) revealed Hg aggregates in hepatic lysosomes. Because dolphins with hepatic lipofuscinosis had higher hepatic mean total Hg concentrations than those without pigment deposits, these authors suggested a causal relationship between hepatic Hg concentrations, lipofuscin accumulation, and hepatic disease (31).

Autometallography (AMG) uses the ability of metal [complexed with either Se or sulfur (S)] in tissue to catalyze a change of silver (Ag) in a physical developer from ionic (Ag^{+}) to metallic form (Ag^{0}). Resultant metallic silver grains appear black and can be visualized at the light microscopic level. Because the silver crystal lattices may be constructed upon a few molecules, the technique serves both to localize as well as amplify the presence of the metal intracellularly (9, 10, 11, 13); thus, the technique is considered semiquantitative.

As reported elsewhere (46), beluga whales sampled in conjunction with this study had significantly higher hepatic concentrations of total Hg [mean total Hg = 23.29 and 4.97 ug/g wet weight (ww) in liver and kidney, respectively; n = 24] than bowhead whales, in which liver Hg was consistently low (mean total Hg = 0.06 ug/g ww;

Address correspondence to: Todd M. O'Hara, Department of Wildlife Management, North Slope Borough, PO Box 69, Barrow, Alaska 99723, USA; e-mail: tohara@co.north-slope.ak.us .

0192-6233/02$3.00+$0.00

n = 55). Therefore, tissue sections (liver and kidney) from bowhead whales were used in lieu of controls, because the total Hg (THg) concentrations in their tissues were negligible. This disparity in patterns of tissue mercury accumulation between the 2 whale species is attributable to differences in the trophic levels that they occupy (46). The objectives of the present study were to: (a) localize and describe the distribution of Hg in kidney and liver of beluga and bowhead whales through light microscopic sections developed using autometallography (AMG); (b) compare AMG staining density in beluga and bowhead livers with concentrations of Hg obtained through standard chemical analysis (46); and (c) compare the hepatic distribution of Hg to that of lipofuscin among beluga whales.

MATERIALS AND METHODS

Sample collection and processing, as well as mercury analysis through cold vapor atomic absorption spectrophotometry (CVAAS) have been described previously (46). Kidney and liver specimens from beluga (kidney, n = 19; liver, n = 20) and bowhead whales (n = 5) were AMG-developed. Sections (3 um) were mounted on 0.5% gelatin-coated (Fisher Scientific, Pittsburgh, PA, USA) slides and deparaffinized. Slides were hydrated in distilled water (30 minutes) prior to AMG development and immersed in 0.05 N HCl (30 minutes) to remove zinc sulfide (13). For liver sections, this was followed by treatment with 1.0% aqueous potassium cyanide (KCN) to remove Ag without affecting Hg or Au (12). After several rinses with distilled water, slides were AMG-developed following the procedure of Gallyas (18). All chemicals were obtained from Sigma Chemical Co (St. Louis, MO, USA) and slides were developed simultaneously to minimize variability. Following AMG development, some slides were routinely counterstained with hematoxylin and eosin. Liver sections to be examined for lipofuscin localization using fluorescent microscopy remained unstained. Identity of golden-brown intracellular pigments also was confirmed as lipofuscin through a series of special stains (44).

AMG-developed slides of beluga and bowhead livers were examined using light microscopy. In beluga hepatic lobules, AMG staining intensity was measured: adjacent to the portal triad (Z1); midway between the portal triad and central vein (Z2); and adjacent to the central vein (Z3). In each of these oil-immersion fields, AMG staining intensity was quantified through computer-assisted densitometry using a system equipped with a Leitz microscope (E. Leitz, Inc, Rockleigh, NJ, USA), along with a Photometrics Image Point digital camera and Image Pro software (Media Cybernetics, Silver Spring, MD, USA). Measurements were taken for 5 randomly selected, intact lobules in 1 tissue section from each animal. The AMG-stained granules were digitally outlined and the same oil-immersion field was examined under fluorescent microscopy with an excitation wavelength of 355–425 nm and suppression at 460 nm, at which band lipofuscin fluoresces yellow to gold (6). Digital photomicrographs were taken and outlines of AMG-stained granules were overlain upon images obtained with fluorescent microscopy to compare localization of inorganic Hg complexes in situ with lipofuscin deposits.

AMG staining densities were square-root transformed and compared among hepatic zones (Z1, Z2, and Z3) and lobules (replicates) within belugas using repeated measures analysis with age (GLGs) as a covariate. Following Conover (7), overall mean AMG staining intensities measured digitally (ie, area occupied by AMG granules in um^2) for each beluga liver were ranked and compared with Hg concentrations and animal ages (GLGs) using Pearson's correlation with Systat (SPSS, Inc, 1998, Chicago, IL, USA) computer software and a significance level of $p < 0.05$.

RESULTS

General Histopathologic Findings

General histopathologic findings among the animals sampled for this studied have been described (44); therefore, only observations germane to the tissues sampled for this study are described briefly herein. All 5 bowhead whale kidneys examined had a generalized, either mild or moderate, noninflammatory periglomerular and interstitial renal fibrosis; 4 whales had incidental mild, renal lithiasis. Livers from all bowheads showed moderate to severe postmortem changes, with bacterial growth frequently present.

The majority of beluga kidneys exhibited mild (n = 12) or moderate (n = 2) Bowman's capsular fibrosis, sometimes accompanied by a mild increase in mesangial matrix. Seven whales had incidental, mild renal lithiasis. Histopathologic changes observed in beluga livers included: diffuse hepatocellular atrophy (n = 9), multifocal telangiectasia (n = 11), and focal or multifocal fibrosis (n = 7), which was accompanied by bile duct proliferation in 3 whales. Mild, patchy inflammation was observed in the liver of 1 whale, and 2 others had mild periportal hepatitis.

AMG Development

None of the bowhead kidney specimens stained for Hg with AMG, consistent with the extremely low tissue concentrations found via chemical analyses (mean THg = 0.025 ug/g ww ± 0.010; n = 5). AMG-developed kidney sections from 19 belugas had a consistent pattern of Hg deposition. In general, specimens from younger belugas had less AMG staining than those from older belugas. In whales with lower tissue Hg concentrations (generally younger animals), AMG granules reflecting Hg localization occurred in the cortical tubular epithelium. AMG granule deposition among whales with higher tissue Hg concentrations (generally older animals) extended to the epithelium of medullary tubules and collecting ducts. In all cases, AMG granules were observed exclusively in the epithelial cytoplasm, presumably as a consequence of lysosomal storage.

As in the kidney, bowhead whale liver specimens exhibited no AMG staining for Hg consistent with the low concentrations of total mercury determined analytically (mean total mercury = 0.025 ug/g ww ± 0.012); nevertheless, abundant hepatic lipofuscin deposition was evident with fluorescent microscopy. Ages of beluga whales, hepatic Hg and Se concentrations and AMG staining densities are summarized in Table 1. Areas occupied by AMG granules correlated significantly with age (r = 0.628; $p = 0.009$; n = 16), concentrations of all forms of Hg determined analytically [ie, total Hg measured directly (THg), total Hg calculated as the sum of divalent mercury and methylmercury (SHg), divalent

TABLE 1.—Ages (in GLGs), mercury and selenium concentrations (ug/g ww), and AMG staining density (um^2) for livers of Alaskan beluga whales.

Animal ID[b]	GLGs[c]	THg[d]	Hg(II)[e]	MHg[f]	SHg[g]	Se	Mean AMG stained area (um^2)[a]			
							Z1	Z2	Z3	Grand mean
BDL-1-97	NA[h]	11.60	13.22	1.53	14.75	13.41	207	235	177	206
BDL-2-97	NA[h]	7.35	8.76	1.93	10.69	5.69	248	120	17	128
BDL-3-97	NA[h]	5.24	4.27	1.02	5.29	6.76	244	116	13	125
HDL-1-97	17	13.00	4.64	1.05	5.69	22.11	361	191	182	245
HDL-2-97	29	18.00	10.46	1.93	12.39	25.77	212	224	63	166
HDL-3-97	25	9.31	11.41	1.38	12.79	9.72	270	79	21	123
HDL-4-97	15	34.60	11.50	1.39	12.89	62.76	220	227	254	234
HDL-5-97	18	50.00	35.55	2.02	37.75	41.88	328	348	343	340
HDL-6-97	26	5.17	3.13	1.47	4.60	44.67	132	3	3	46
HDL-7-97	7	1.85	0.64	0.52	1.15	9.93	0	0	0	0
HDL-14-97	3	0.33	0.11	0.19	0.29	3.66	0	0	0	0
KDL-1-97	NA[h]	9.15	4.61	0.99	5.60	7.78	174	54	12	80
LDL-3-96	34	73.50	11.58	2.96	14.54	57.53	393	379	159	310
LDL-8-96	12	6.66	2.67	1.32	4.18	17.78	287	2	2	97
LDL-10-96	16	12.27	6.62	1.87	8.50	13.17	176	71	55	101
LDL-13-96	33	2.61	20.75	1.66	22.41	32.57	123	144	67	111
LDL-14-96	14	5.04	2.12	1.07	3.19	13.33	77	14	7	33
LDL-15-96	44	82.47	21.25	1.73	22.98	85.67	406	478	401	428
LDL-24-96	35	83.36	25.61	2.10	27.71	69.85	179	246	193	206
LDL-29-96	46	35.12	9.01	3.89	12.89	63.25	151	210	178	180

[a] Mean AMG-stained area (um^2) is given for: periportal zones (Z1), midzonal areas (Z2), and pericentral zones (Z3; n = 5 liver lobules for each animal); a grand mean is then shown for all 3 zones across 5 liver lobules (n = 5 liver lobules ×3 zones for each = 15 total AMG area counts from which the grand mean was determined for each animal's liver).
[b] Animal ID designations contain references to: harvest location (B = Barrow; H = Pt. Hope; K = Kaktovik; L = Pt. Lay), species (*D. leucas*), year sampled, and sample number (ie, LDL-3-96 was the third beluga whale examined in 1996 in Pt. Lay).
[c] Growth layer groups (estimated to be 2 GLGs/year).
[d] Total Hg determined directly.
[e] Inorganic Hg.
[f] Monomethyl Hg.
[g] Total Hg calculated [SHg = Hg(II) + MHg].
[h] Not available.

mercury (Hg(II)), and methylmercury (MHg)] (Table 2). Concentrations of MHg and Se were less strongly correlated with AMG granule densities than were measures of total Hg or inorganic Hg (Table 2), although all were significant. Among belugas, a difference in AMG granule density was observed between zones of hepatic lobules ($p = 0.03$). In general, hepatic sections from younger animals contained markedly fewer AMG granules than those from older whales. For example, the youngest whale sampled (3 GLGs of age), had hepatic Hg concentrations similar to the bowheads, and also displayed no AMG staining. In belugas with lower tissue concentrations of Hg (usually younger whales), AMG granules were most concentrated around portal triads (Z1). Whales with intermediate concentrations of hepatic Hg had AMG granules near portal triads (Z1), as well as around central veins (Z3). Sections from belugas with the highest hepatic concentrations of Hg (usually older animals) exhibited AMG granule deposition around portal triads (Z1), central veins (Z3), and in the parenchyma between these landmarks (Z2).

TABLE 2.—Pearson's correlation matrix (followed by associated *p*-values in parentheses) for mean area occupied by AMG granules (um^2) and tissue concentrations (ug/g ww) of mercury and selenium in livers of Alaskan beluga whales (n = 20).

	Mean AMG-stained area	THg[a]	Hg(II)[b]	MHg[c]	SHg[d]	Se
THg	0.88 (<0.001)	1.00				
Hg(II)	0.81 (<0.001)	0.75 (<0.001)	1.00			
MHg	0.62 (0.004)	0.71 (<0.001)	0.72 (<0.001)	1.00		
SHg	0.81 (<0.001)	0.76 (<0.001)	0.99 (<0.001)	0.76 (<0.001)	1.00	
Se	0.63 (0.003)	0.70 (0.001)	0.62 (0.003)	0.63 (0.003)	0.65 (0.002)	1.00

[a] Total Hg determined directly.
[b] Inorganic Hg.
[c] Monomethyl Hg.
[d] Total Hg calculated [SHg = Hg(II) + MHg].

As a rule, we observed AMG granules in beluga liver sections in 2 cellular locations. Large granular aggregates were observed in stellate macrophages (Kupffer cells), especially near portal triads (Z1; Figure 1). Granules also were observed in hepatocellular cytoplasm, and often appeared in almost linear arrays toward the centers of hepatic cords, corresponding with the bile cannalicular domains of the cells. Granules were discrete, indicating that Hg was most likely confined within lysosomes.

Lipofuscin Distribution (Fluorescent Microscopy)

In AMG-developed sections, lipofuscin appeared as yellow-to-gold fluorescent foci and was abundant in all livers, including those from bowhead whales and young belugas with little to no AMG staining (reflecting low hepatic Hg concentrations). Although lipofuscin also was present among belugas with higher hepatic concentrations of Hg, it did not exist in noticeably greater amounts than in livers of animals containing minimal Hg. Whereas AMG granules appeared to accumulate primarily around portal triads (Z1), lipofuscin was most prominent pericentrally (Z3). Lipofuscin deposits varied in morphology, appearing lemon-yellow and rather diffuse periportally (Z1) and becoming increasingly condensed and golden with progression to pericentral zones (Z3). As with AMG granules, lipofuscin granules were often in central linear arrays within hepatic cords, associated with the bile cannalicular hepatocellular domain. Although AMG

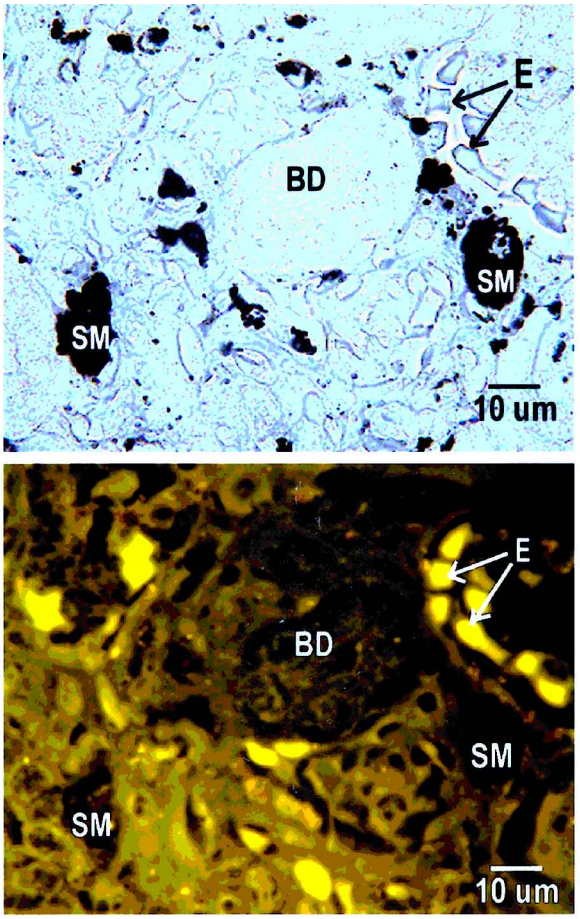

FIGURE 1.—Periportal region of a beluga liver developed with autometallography, under light (top) and fluorescent (bottom) microscopy. Bile duct, BD; erythrocyte, E; lipofuscin, L; and stellate macrophage, SM.

and lipofuscin were sometimes colocalized, most often they occurred independently.

DISCUSSION

In general, histopathologic changes observed in liver and kidney of bowhead and beluga whales were noninflammatory and not clinically significant. The etiology of hepatic atrophy was believed to be nutritional because it was often accompanied by pancreatic involution and coincided with a prevailing lack of stomach contents.

AMG Development

Whereas AMG has been used extensively to detect deposits of Timm-reactive metals [ie, metallic gold, as well as sulfides or selenides of Ag, zinc (Zn), and Hg] in controlled experiments (1, 2, 8, 12, 13), and in domesticated species (19), the application of this technique to localize Hg in situ in tissues from free-ranging cetaceans is novel.

The strong positive correlation of mean AMG granule densities in beluga livers with tissue concentrations of both inorganic and total Hg validates the sensitivity of the AMG staining. Likewise, the finding that MHg and Se were less strongly correlated with AMG granule densities supports the specificity of the staining method. The AMG development will stain only Hg bound to S or Se in tissue (12, 13). Consequently, the minor proportion of Hg present in organic form in beluga livers would not be expected to catalyze AMG development. Because hepatic MHg and Se are mutually correlated with inorganic Hg due to their concurrent bioaccumulation (46), the positive correlation of AMG granule density with both MHg and Se is not surprising. Moreover, the lower correlation coefficients for the association between these molecular species and AMG-stained area in comparison to that for inorganic Hg with AMG-stained area would be expected.

Renal Distribution of AMG Granules

The depositional pattern of AMG granules in beluga whale kidneys of this study is consistent with controlled experiments in laboratory animals documenting the renal disposition of inorganic and organic Hg (48); however, in the belugas the renal tubular distribution was less restricted. In laboratory experiments with rodents, the accumulation and toxic effects (epithelial necrosis and sloughing) of both organic and inorganic Hg appear to be confined to the proximal tubule (16, 17, 20, 23), with most marked effects on the epithelium of the pars recta (straight segment) at the corticomedullary junction (48). In our study of belugas, AMG granules reflecting Hg deposition were observed in epithelia of both proximal and distal tubules in renal cortex, as well as in epithelia of uriniferous tubules throughout renicular medullary and papillary zones [ie, in intermediate tubules (formerly known as loops of Henle) and collecting ducts, respectively]. Hansen and Danscher (19) remarked a like pattern of inorganic Hg deposition in kidneys of sledgedogs that had been maintained on diets high in marine mammal tissues, in which Hg deposition was apparent throughout the nephron, especially in the lysosomes of the proximal tubular cells.

The AMG granules indicating Hg niduses in uriniferous tubular epithelial cytoplasm probably occurred within lysosomes. Although Hg has been found to disseminate through all intracellular pools of proximal tubular epithelial cells (48), a predominantly lysosomal pattern of distribution is consistent with chronic Hg exposure (27). Although the mechanism of lysosomal Hg accumulation is unknown, it might result from autophagy of cytoplasmic Hg bound to cellular organelles or endogenous ligands such as metallothionein (27). In this context, lysosomal sequestration, presumably followed by digestion of organic ligands and extrusion of Hg (either bound to endogenous ligands or sequestered in sloughed epithelial cells) into the renal tubular lumen, may serve a protective and excretory role. Alternatively, lysosomal Hg accretion may occur through endocytic uptake of filtered, protein-bound Hg (20). Such absorption could culminate in excretion, as previously mentioned, or mediate cytotoxic effects (17, 20).

Among belugas in this study, the presence of Hg in epithelial cells in all portions of the uriniferous tubule suggests that its accumulation results largely through diffusion from interstitial fluid or blood rather than by absorption from luminal filtrate, which is confined to the proximal tubule. Thus, it is likely that the AMG-stained Hg is bound to endogenous ligands—most likely S- or Se-containing molecules, potentially including metallothionein—and packaged as autophagic lysosomes for eventual excretion. Both inorganic and organic forms of Hg can decrease lysosomal enzymatic activity as well as associated protein catabolism

(17, 26), which may increase susceptibility of the uriniferous tubular epithelium to other insults (17), or perhaps result in the observed epithelial accumulation of Hg.

Hepatic Distribution of AMG Granules

In beluga liver sections, AMG granules exhibited marked zonal distribution, apparently reflecting initial accumulation around portal triads with progressive dissemination throughout all 3 lobular zones as hepatic Hg concentrations increase with age. This lobular zonation confirms that Hg is not simply homogenously distributed throughout the hepatic parenchyma. Similarly, Berlin and Ullberg (4) documented a periportal distribution of Hg via autoradiography in mice following a single intravenous injection of $Hg^{203}Cl_2$. Although the restriction of AMG granules to hepatocytes and macrophages was similar between the beluga whales and sledgedogs on marine mammal diets (19), the periportal aggregation of AMG granules in belugas contrasts with the findings in sledgedogs, in which Hg-catalyzed AMG granules invariably aggregated most densely in centrilobular regions of the liver (19), suggesting interspecific variation in mechanisms of Hg disposition.

Baatrup et al (2) used AMG staining of Hg in livers of rats treated with either MHg or Hg(II) alone, or followed by treatment with Se. In rats given Hg(II) alone, staining was seen predominantly in Kupffer cells (stellate macrophages), with only scant amounts detected in endothelial cells and hepatocytes. However, when Se followed Hg(II) treatment, AMG staining within hepatocytes (including their nuclei), endothelial cells and erythrocytes increased dramatically (2). In rats given MHg alone, no AMG staining was observed, but when Se administration followed MHg treatment, AMG staining was concentrated in Kupffer cell cytoplasm and endothelial cells, with lesser amounts in cytoplasm of hepatocytes (2). These findings emphasize the complicated hepatic toxicodistribution of Hg based on the predominant form of Hg (inorganic vs organic), and the interaction of Hg with other elements, such as Se.

Among belugas in this study, Hg-catalyzed AMG granules were amassed in greatest numbers in stellate macrophages and also dispersed in hepatocytic cytoplasm, apparently confined to lysosomes, which frequently were clustered in the bile cannalicular domain of the cells.

Baatrup et al (2) results, in conjunction with our observations suggest that the formation of the AMG granules in beluga livers was probably catalyzed by Hg interacting with Se. This supposition is supported by previous research that has shown a strong positive correlation between tissue concentrations of these elements (15, 24, 25, 41, 46). Furthermore, the absence of granules in endothelial cells of beluga liver, as well as the likely restriction of granules to lysosomal compartments in stellate macrophages and hepatocytes, implies that binding to vital cellular organellar components (such as mitochondria or nuclei) is minimal in this species. In light of the previously described differences in AMG granule deposition between Hg(II)- and MHg-treated rats found by Baatrup et al. (2), the cellular and intracellular pattern of AMG-granule deposition in the present study, in addition to the absence of granules in hepatocytic nuclei, suggest that the majority of Hg present was originally in organic form, which is consistent with some food web sources (32).

The aggregation of AMG granules in macrophages attests to the importance of these cells in Hg toxicodisposition. Degenerative hepatocytes likely release cytoplasmic HgSe complexes into the bloodstream, which would presumably be phagocytized by macrophages. How these macrophages contend with this internalized inorganic material is not known. Interestingly, preliminary data from belugas in this study showed that appreciable concentrations of THg (~5 ug/g ww) occurred in mesenteric lymph nodes, yet among ringed seals, nodal THg was minimal (Woshner and Bratton, unpublished data). Suda and Takahashi (35) suggested that the reticuloendothelial system might represent the main site for degradation of MHg to inorganic Hg. Their premise was bolstered by a survey of tissues from Greenlandic sledgedogs on diets of marine mammal tissues, in which the highest Hg concentrations were found in mesenteric lymph nodes (19). The prospect that macrophages constitute a crucial mode of Hg detoxification certainly should be considered and investigated further with respect to belugas and other odontocetes.

Lipofuscin

Lipofuscin, often termed an age pigment, is a heterogeneous, autofluorescent pigment believed to result from peroxidation of unsaturated fatty acid components of membranous organelles (21, 22). Lipofuscin consists of polymerized, oxidized lipids with some protein constituent (6, 30, 34) and its formation reflects oxidative stress and associated intracellular damage, although not necessarily of sufficient magnitude to impair form or function. Rather, it accumulates in a variety of tissues and cell types as a normal consequence of aging-related processes, and may represent products of various cellular defense mechanisms that protect against free radicals (33, 47). The golden-brown intracellular pigment observed in beluga and bowhead whale tissue sections fluoresced at a wavelength consistent with that of lipofuscin, corroborating light microscopic observations and identification (44). Although Hg-catalyzed AMG granules and lipofuscin were sometimes colocalized, they more often were not. Furthermore, bowhead and young beluga whales with low hepatic Hg concentrations (for example, HDL-7-97 and HDL-14-97 with hepatic THg concentrations of 1.85 and 0.33 ug/g ww, respectively) exhibited abundant hepatic lipofuscin deposition. In beluga livers, lipofuscin appeared most abundant pericentrally, which is typical for domesticated species as well (22). This contrasted with the prevailing configuration of Hg-induced AMG granules, which tended to concentrate in periportal zones. These findings indicate that hepatic lipofuscin is a common, normal finding in these animals, and probably is not directly related to hepatic Hg accumulation as proposed by Rawson et al (31) in dolphins.

Although evident that lipofuscin accumulation is a common finding in apparently healthy, free-ranging whales, the underlying mechanisms and implications of its presence remain unclear. This is largely because the significance of lipofuscin itself is not well understood in general. It is widely accepted that lipofuscin forms as a consequence of intracellular damage and may be promulgated by a variety of etiologies, including dietary unsaturated lipids, anti-oxidant deficiencies and chronic hypoxia, among others (14, 30). However, the consequences of lipofuscin accumulation are disputed, and some researchers have contended that the pigment itself is

damaging (21). It has been suggested that autophagocytosis and compromised lysosomal function occur with age-related lipofuscin accumulation (38, 39), which acts as a cellular stressor (37, 47). In the current study, however, cells with abundant lipofuscin deposition (hepatocytes, macrophages) appeared normal and healthy histologically.

In conclusion, based on visualization of AMG granules in this study, Hg appears to accumulate in precise areas of beluga liver and kidney. Specifically, in liver Hg was restricted to cytoplasm of hepatocytes and stellate macrophages and most concentrated in periportal followed by pericentral zones, whereas in kidney Hg was confined to the cytoplasm of uriniferous tubular epithelium—especially that of cortical tubules. Moreover, the tissular localization of Hg (as indicated by AMG granules) and the age-associated accumulation of Hg do not appear to be directly related to lipofuscin accumulation in the beluga liver. Rather, the preponderance of lipofuscin probably reflects diet and the tremendous oxidative stress of their existence, and may provide important clues for assessing beluga oxidative status and mechanisms of defense. Indeed, it may be that cetacean adaptations to a high degree of oxidative stress imposed by diet and habitat have allowed them, as a fortuitous side-effect, to tolerate greater exposures to toxic metals, without precipitating clinical toxicosis, than might be sustained by terrestrial mammals.

ACKNOWLEDGMENTS

We are grateful to Dr. Bob Switzer, Neuroscience Associates, Knoxville, TN, for the AMG protocol, to Dr. David Schaeffer, for help with statistical analysis, and to Charles D.N. Brower, Director, and other personnel of the Department of Wildlife Management, North Slope Borough, for their support. We extend special thanks to the subsistence hunters of Pt. Hope, Pt. Lay, Barrow, and Kaktovik (Alaska) for permitting us to sample their animals.

This project was funded primarily by the Office of Naval Research to the North Slope Borough. Additional support was provided by the Alaska Beluga Whale Committee, North Slope Borough, and the Office of the Epidemiologist, State of Alaska.

REFERENCES

1. Baatrup E, Danscher G (1987). Cytochemical demonstration of mercury deposits in trout liver and kidney following methyl mercury intoxication: Differentiation of two mercury pools by selenium. *Ecotoxicol Environ Saf* 14: 129–141.
2. Baatrup E, Thorlacius-Ussing O, Nielsen H, Wilsky K (1989). Mercury-selenium interactions in relation to histochemical staining of mercury in the rat liver. *Histochem J* 21: 89–98.
3. Becker P, Mackey E, Demiralp R, Schantz M, Koster B, Wise S (1997). Concentrations of chlorinated hydrocarbons and trace elements in marine mammal tissues archived in the U.S. National Biomonitoring Specimen Bank. *Chemosphere* 34: 2067–2098.
4. Berlin M, Ullberg S (1963). Accumulation and retention of mercury in the mouse. *Arch Environ Health* 6: 589–601.
5. Chio K, Tappel A (1969). Synthesis and characterization of the fluorescent products derived from malonaldehyde and amino acids. *Biochemistry* 8: 2821–2826.
6. Christensen M, Rungby J, Mogensen S (1989). Effects of selenium on toxicity and ultrastructural localization of mercury in cultured murine macrophages. *Toxicol Lett* 47: 259–270.
7. Conover WJ (1971). *Practical Nonparametric Statistics*. Wiley, New York.
8. Danscher G (1991). Applications of autometallography to heavy metal toxicology. *Pharmacol Toxicol* 69: 414–423.
9. Danscher G (1981). Light and electron microscopic localization of silver in biological tissue. *Histochemistry* 71: 177–186.
10. Danscher G, Hansen H, Møller-Madsen B (1984). Energy dispersive X-ray analysis of tissue gold after silver amplification by physical development. *Histochemistry* 81: 283–285.
11. Danscher G, Møller-Madsen B (1985). Silver amplification of mercury sulfide and selenide: A histochemical method for light and electron microscopic localization of mercury in tissue. *J Histochem Cytochem* 33: 219–228.
12. Danscher G, Rungby J (1986). Differentiation of histochemically visualized mercury and silver. *Histochem J* 18: 109–114.
13. Danscher G, Stoltenberg M, Juhl S (1994). How to detect gold, silver and mercury in human brain and other tissues by autometallographic silver amplification. *Neuropathol Appl Neurobiol* 20: 454–457.
14. de Gritz B, Rahko T (1995). Diet-induced residual formation in pigs. *Gerontology* 41: 305–315.
15. Dietz R, Nielsen C, Hansen M, Hansen CT (1990). Organic mercury in Greenland birds and mammals. *Sci Total Environ* 95: 41–51.
16. Fowler B (1972). Ultrastructural evidence for nephropathy induced by long-term exposure to small amounts of methyl mercury. *Science* 175: 780–781.
17. Fowler B, Brown H, Lucier G, Krigman MR (1975). The effects of chronic oral methyl mercury exposure on the lysosome system of the rat kidney. *Lab Invest* 32: 313–322.
18. Gallyas F (1979). Light insensitive physical developers. *Stain Technol* 54: 173–176.
19. Hansen J, Danscher G (1995). Quantitative and qualitative distribution of mercury in organs from arctic sledgedogs: An atomic absorption spectrophotometric and histochemical study of tissue samples from natural long-termed high dietary organic mercury-exposed dogs from Thule, Greenland. *Pharmacol Toxicol* 77: 189–195.
20. Hultman P, Enestrom S, von Schenck H (1985). Renal handling of inorganic mercury in mice. *Virchows Arch* B49: 209–224.
21. Jones TC, Hunt RD, King NW (1997). *Veterinary Pathology*, 6th ed, Lippincott Williams & Wilkins, Baltimore, Maryland.
22. Jubb KVF, Kennedy PC, Palmer N (1993). *Pathology of Domestic Animals*, 4th ed, Vol 2. Academic Press, San Diego, California.
23. Klein R, Herman S, Bullock B, Talley F (1973). Methyl mercury intoxication in rat kidneys. *Arch Pathol* 96: 83–90.
24. Koeman J, Peeters W, Koudstaal-Hol C, Tijoe P, De Goeij J (1973). Mercury-selenium correlations in marine mammals. *Nature* 245: 385–386.
25. Koeman J, van de Ven W (1975). Mercury and selenium in marine mammals and birds. *Sci Total Environ* 3: 279–287.
26. Madsen K, Christensen EI (1978). Effects of mercury on lysosomal protein digestion in the kidney proximal tubule. *Lab Invest* 38: 165–174.
27. Madsen K, Hansen JC (1980). Subcellular distribution of mercury in the rat kidney cortex after exposure to mercuric chloride. *Toxicol Appl Pharmacol* 54: 443–453.
28. Martoja R, Berry J (1980). Identification of tiemannite as a probable product of demethylation of mercury by selenium in cetaceans. A complement to the scheme of the biological cycle of mercury. *Vie Millieu* 30: 7–10.
29. Nigro M, Leonzio C (1996). Intracellular storage of mercury and selenium in different marine vertebrates. *Marine Ecology-Progress Series* 135: 137–143.
30. Porta E, Hartroft W (1969). Lipid pigments in relation to aging and dietary factors (lipofuscins). In: *Pigments in Pathology*, Wolman M (ed). Academic Press, New York, pp 191–235.
31. Rawson A, Patoon G, Hofmann S, Pietra G, Johns L (1993). Liver abnormalities associated with chronic mercury accumulation in stranded Atlantic bottlenose dolphins. *Ecotoxicol Environ Saf* 25: 41–47.
32. Rouleau C, Gobeil C, Tjälve H (2000). Accumulation of silver from the diet in two marine benthic predators: The snow crab (*Chionoectetes opilio*) and American plaice (*Hippoglossoides platessoides*). *Environ Toxicol Chem* 19: 631–637.
33. Schwartsburd P (1995). On the origin of heterogeneity of lipofuscin fluorophores and their possible interrelations. *Gerontology* 41: 29–37.

34. Shimasaki H, Ueta N, Privett O (1982). Covalent binding of peroxidized linoleic acid to protein and amino acids as models for lipofuscin formation. *Lipids* 17: 878–883.
35. Suda I, Takahashi H (1990). Effect of reticuloendothelial system blockade on the biotransformation of methyl mercury in the rat. *Bull Environ Contam Toxicol* 44: 609–615.
36. Suda I, Totoki S, Takahashi H (1991). Degradation of methyl and ethyl mercury into inorganic mercury by oxygen free radical-producing systems: Involvement of hydroxyl radical. *Arch Toxicol* 65: 129–134.
37. Terman A, Abrahamsson N, Brunk UT (1999). Ceroid/lipofuscin-loaded human fibroblasts show increased susceptibility to oxidative stress. *Exp Gerontol* 34: 755–770.
38. Terman A, Brunk UT (1998). Lipofuscin—Mechanisms of formation and increase with age. *APMIS* 106: 265–276.
39. Terman A, Dalen H, Brunk UT (1999). Ceroid/lipofuscin-loaded human fibroblasts show decreased survival time and diminished autophagocytosis during amino acid starvation. *Exp Gerontol* 34: 943–957.
40. Wagemann R (1989). Comparison of heavy metals in two groups of ringed seals (*Phoca hispida*) from the Canadian Arctic. *Can J Fish Aquatic Sci* 46: 1558–1563.
41. Wagemann R, Innes S, Richard P (1996). Overview and regional and temporal differences of heavy metals in Arctic whales and ringed seals in the Canadian Arctic. *Sci Total Environ* 186: 41–66.
42. Wagemann R, Snow N, Lutz A, Scott D (1983). Heavy metals in tissues and organs of the narwhal (*Monodon monoceros*). *Can J Fish Aquatic Sci* 40(Suppl. 2): 206–214.
43. Wagemann R, Stewart R, Beland P, Desjardins C (1990). Heavy metals and selenium in tissues of beluga whales, *Delphinapterus leucas*, from the Canadian Arctic and the St. Lawrence Estuary. *Can Bull Fish Aquatic Sci* 224: 191–206.
44. Woshner VM (2000). Concentrations and interactions of selected elements in tissues of four marine mammal species harvested by Inuit hunters in arctic Alaska, with an intensive histologic assessment, emphasizing the beluga whale. University of Illinois at Urbana-Champaign Urbana, Illinois, PhD Dissertation.
45. Woshner VM, O'Hara TM, Bratton GR, Beasley VR (2001). Concentrations and interactions of selected essential and non-essential elements in ringed seals and polar bears of arctic Alaska. *J Wildl Dis* 37(4): 711–721.
46. Woshner VM, O'Hara TM, Bratton GR, Suydam RS, Beasley VR (2001). Concentrations and interactions of selected essential and non-essential elements in bowhead and beluga whales of arctic Alaska. *J Wildl Dis* 37(4): 693–710.
47. Yin D (1995). Studies on age pigments evolving into a new theory of biological aging. *Gerontology* 41: 159–170.
48. Zalups R, Lash LH (1994). Advances in understanding the renal transport and toxicity of mercury. *J Toxicol Environ Health* 42: 1–44.